Electronic Supplementary Material (ESI) for New Journal of Chemistry.

Electronic Supplementary Information (ESI)

SYNTHESIS OF NOVEL AIEE ACTIVE PYRIDOPYRAZINES AND THEIR APPLICATIONS AS CHROMOGENIC AND FLUOROGENIC PROBES FOR Hg^{2+} DETECTION IN AQUEOUS MEDIA

Shalu Gupta, Marilyn D. Milton*

Department of Chemistry, University of Delhi, Delhi 110007, India

*Corresponding author. Tel.: +91 11 27667794 *Extn.* 140.

E-mail address: mdmilton@chemistry.du.ac.in

Contents:

General method for preparation of solutions for fluorescence and absorption measurements:

The stock solutions of 2×10^{-3} M concentration of synthesized compounds were prepared in HPLC acetonitrile and diluted accordingly. All the studies were performed in non-buffered media. 0.015 M stock solution of metal salts were prepared in HPLC water and diluted accordingly. For AIEE studies 0.15 mL of stock solution was taken and diluted accordingly acetonitrile & water. While determining selectivity of interaction of probes with metal ion, titrations were performed by adding 0.1 mL of metal salt solutions to 3 mL solutions of probes. The binding stoichiometry was determined by Job's plot experiments.

Determination of detection Limit:-

The detection limit was calculated using fluorescence titration spectra. The detection limit of probe PP-Hg for Hg^{2+} was determined from the followingequation:

$$DL = 3S/b \qquad \textbf{Equation S1}$$

where S is the standard deviation of blank measurements, *b* is the slope of fluorescence intensity versus concentration Hg^{2+}.[1] Where standard deviation is calculated using the formula

$$S = \sqrt{\frac{\sum(Io - I)^2}{N - 1}}$$

I_0 is the fluorescence intensity of probe and I isaverage of the I_0.

The calculation of association constant (K_a)

For 1:n stoichiometry between chemosensor and metal ion, the Benesi-Hildebrand equation could be derived as:[2]

$$\frac{1}{I - I_0} = \frac{1}{K_a(Imax - I_0)[M]_0^n} + \frac{1}{Imax - I_0} \qquad \textbf{Equation S2}$$

Where I is the intensity of chemosensor at the maximum absorption wavelength after treatement with metal ion, I_{max} is the largest intensity of chemosensor at the maximum absorption

wavelength with excess amount of metal ion, I_0 is the initial intensity of chemosensor, [M] is the concentration of metal ion-added, $K_a$is the association constant and n is the stoichiometricratio.

Table S1. Crystal data and structure refinement for probe **PP1.**

Empirical formula	C_{34} H_{20} Cl_3 N_5
Formula weight	604.90
Temperature	298 K
Wavelength	0.71073 Å
Crystal system	Monoclinic
Space group	P $_{1\,21}$/n $_1$
Unit cell dimensions	a = 9.0622 (7) Å
	b = 16.3810(13) Å
	c = 19.4841(16) Å
	α= 90.00(7) °
	β=102.514(7)°
	γ= 90.00(6)°
Volume	2823.6(4) $Å^3$
Z	4
Density (calculated)	1.423Mg/m^3
Absorption coefficient	0.359mm^{-1}
F(000)	1240
Crystal size	0.24 x 0.16 x 0.12 mm^3
Theta range for data collection	3.01to 29.40°.

Index ranges	-12<=h<=12, -22<=k<=22, -26<=l<=24
Reflections collected	3110
Independent reflections	7068 [R(int) = 0.0939]
Completeness to theta = 25.242°	99.8 %
Refinement method	Full-matrix least-squares on F2
Data / restraints / parameters	7068 / 0 / 354
Goodness-of-fit on F2	1.022
Final R indices [I>2sigma(I)]	R_1 = 0.0923, wR_2 = 0.1803
R indices (all data)	R_1 = 0.2076, wR_2 = 0.2316
Extinction coefficient	n/a
Largest diff. peak and hole	0.517and -0.497e.$Å^{-3}$

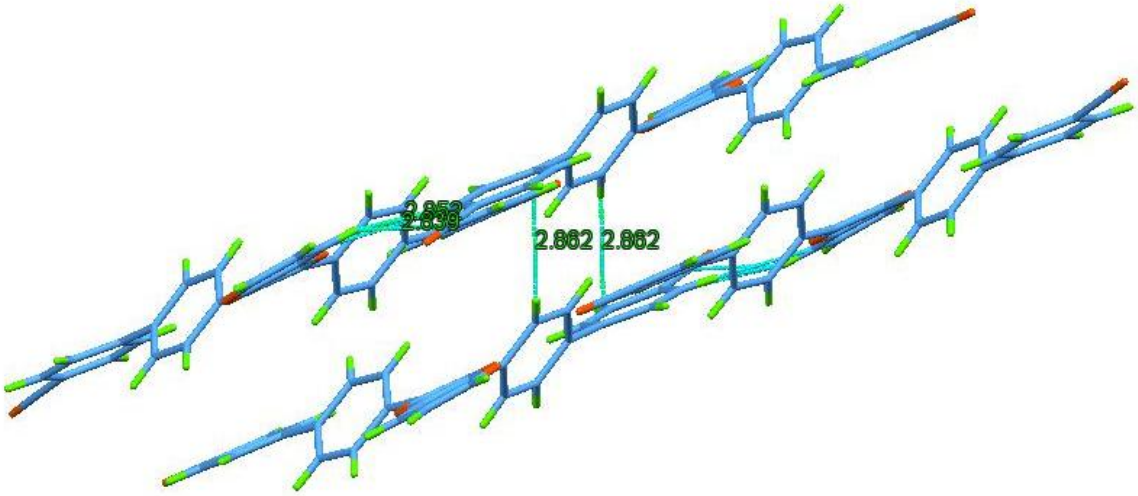

Figure S1. Multiple intermolecular C···H-C, C-C interaction existed in the **PP1.**

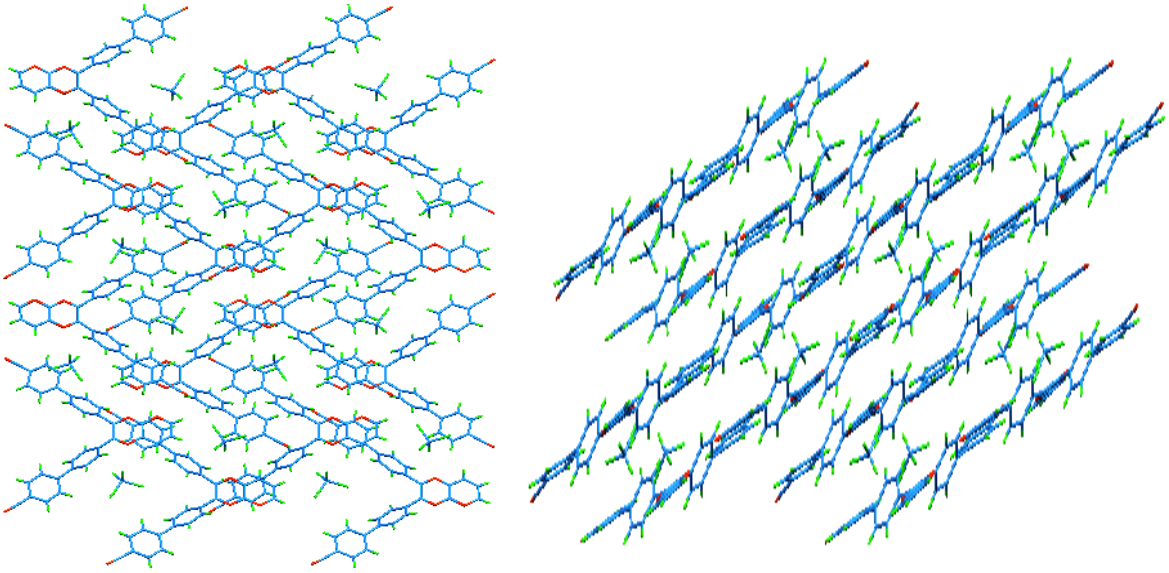

Figure S2. Crystal packing of **PP1** when viewed along (i) *a* axis (ii) *b* axis showing layered arrangement of molecules.

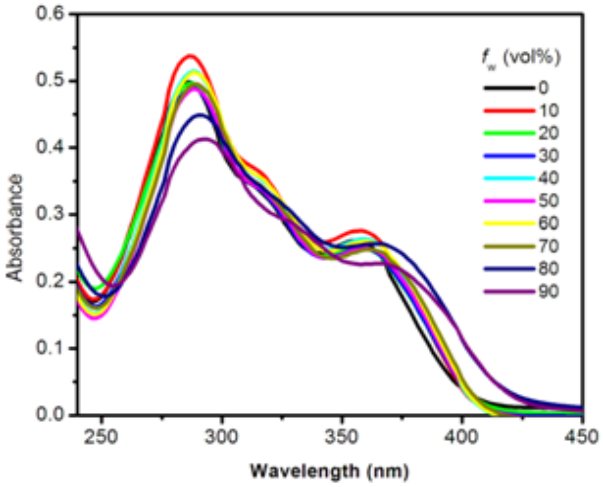

Figure S3. Absorption spectra (10 μM) of**PP1**in H_2O-CH_3CN mixture with different water fractions.

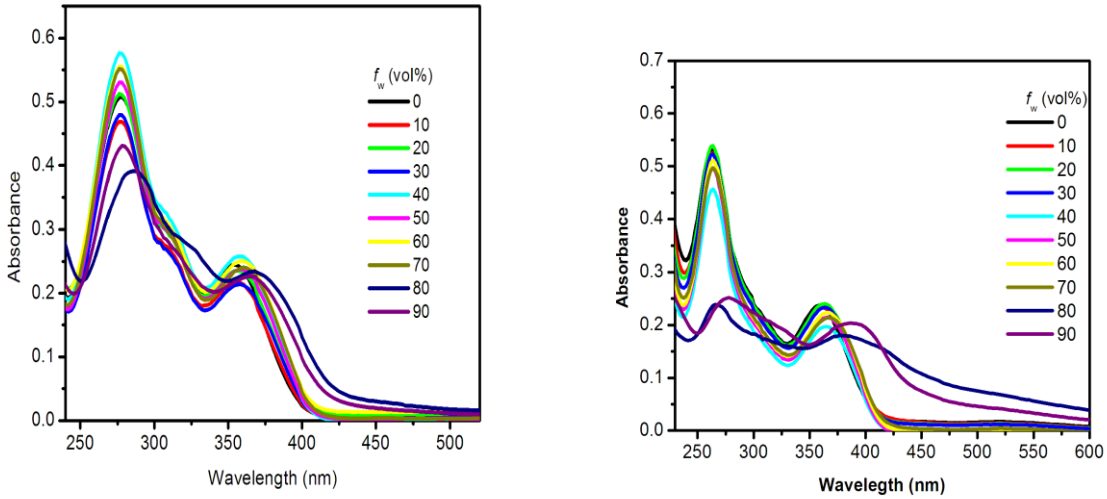

Figure S4. Absorption spectra (10 μM) of (i) **PP2** and (ii) **PP3** in H_2O-CH_3CN mixture with different water fractions.

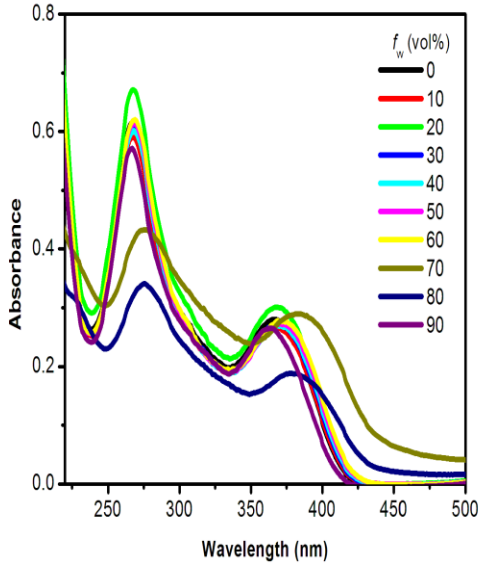

Figure S5. Absorption spectra (10 μM) of **PP4** in H_2O-CH_3CN mixture with different water fractions.

i)

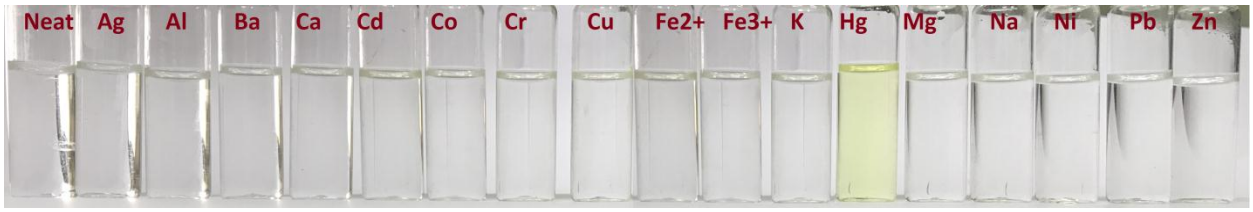

ii)

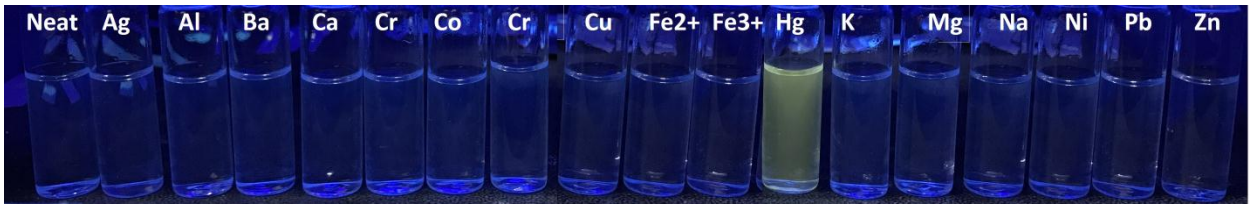

Figure S6. Photographs of solution of probe **PP2** in CH_3CN-H_2O (8:2, v/v) in the presence of various metal ions (10 eq) (from right to left) i) under ambient light ii) under a UV irradiation at 365 nm.

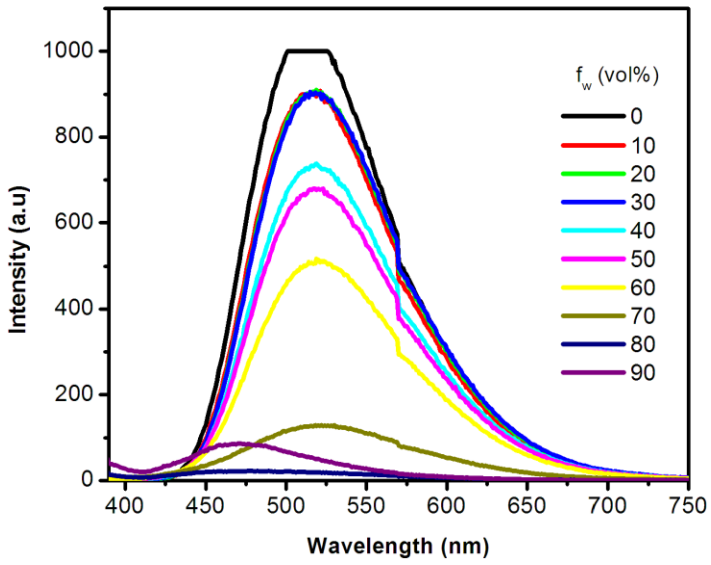

Figure S7. Fluorescence spectra of **PP1**(50 μM) upon addition of Hg^{2+}(10 eq.) in H_2O-CH_3CN mixture with different water fractions (f_w).

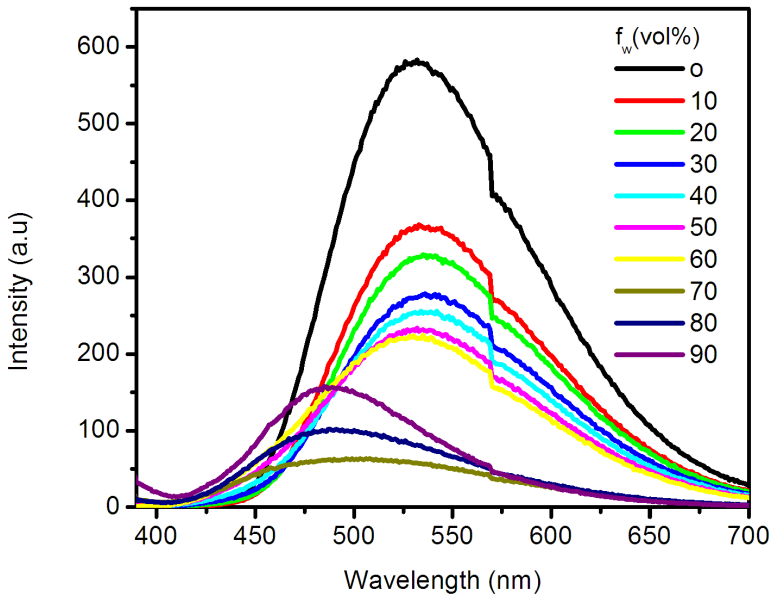

Figure S8. Fluorescence spectra of **PP2** (50 μM) upon addition of Hg^{2+}(10 eq.) in H_2O-CH_3CN mixture with different water fractions (f_w).

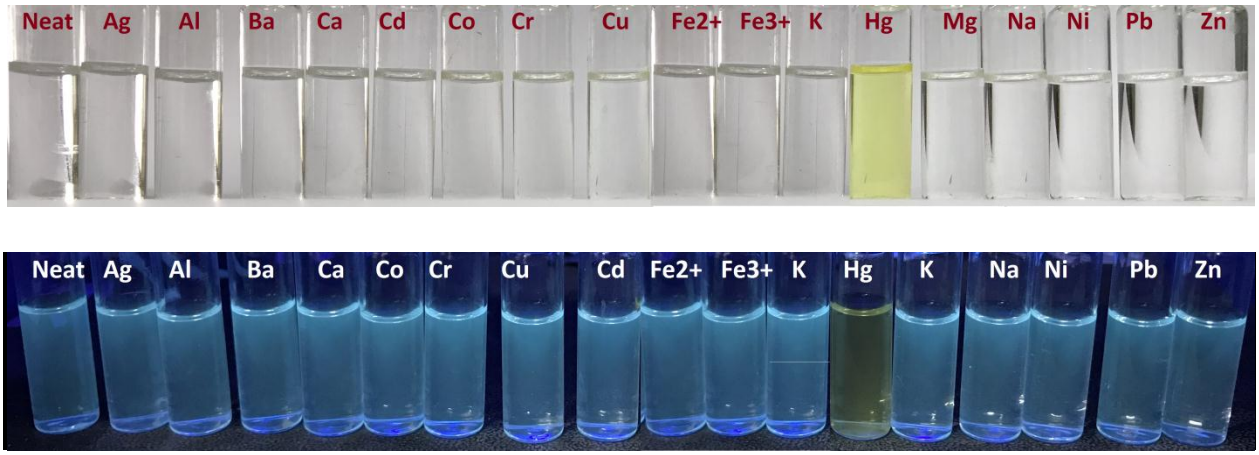

Figure S9. Photographs of solution of probe **PP3** in CH_3CN-H_2O (7:3, v/v) in the presence of various metal ions (10 eq) (from right to left) i) under ambient light ii) under a UV irradiation at 365 nm.

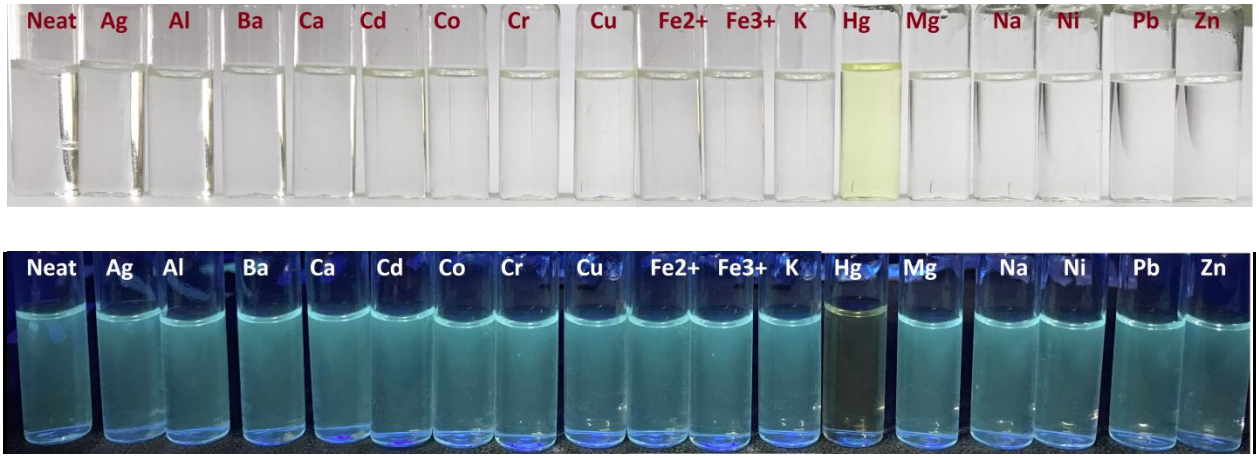

Figure S10. Photographs of solution of probe **PP4** in CH_3CN-H_2O (9:1, v/v) in the presence of various metal ions (10 eq) (from right to left) i) under ambient light ii) under a UV irradiation at 365 nm.

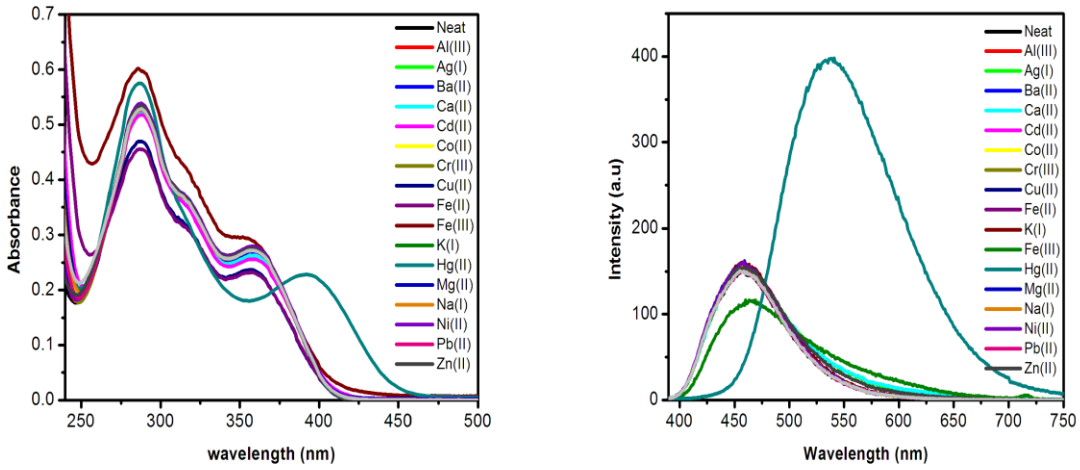

Figure S11.(i) Absorption spectra (10 μM) and (ii) fluorescence spectra (50 μM) of **PP2** in CH_3CN-H_2O (8:2, v/v) on addition of 10eq. of various metal cations (metal nitrates were studied).

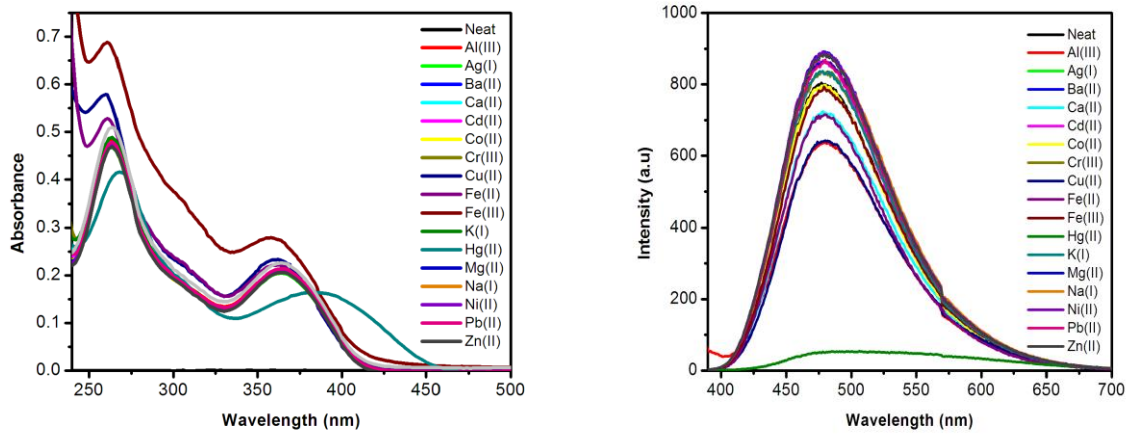

Figure S12. (i) Absorption spectra (10 μM) and (ii) fluorescence spectra (50 μM) of **PP3** in CH_3CN-H_2O (7:3, v/v) on addition of 10eq. of various metal cations (metal nitrates were studied).

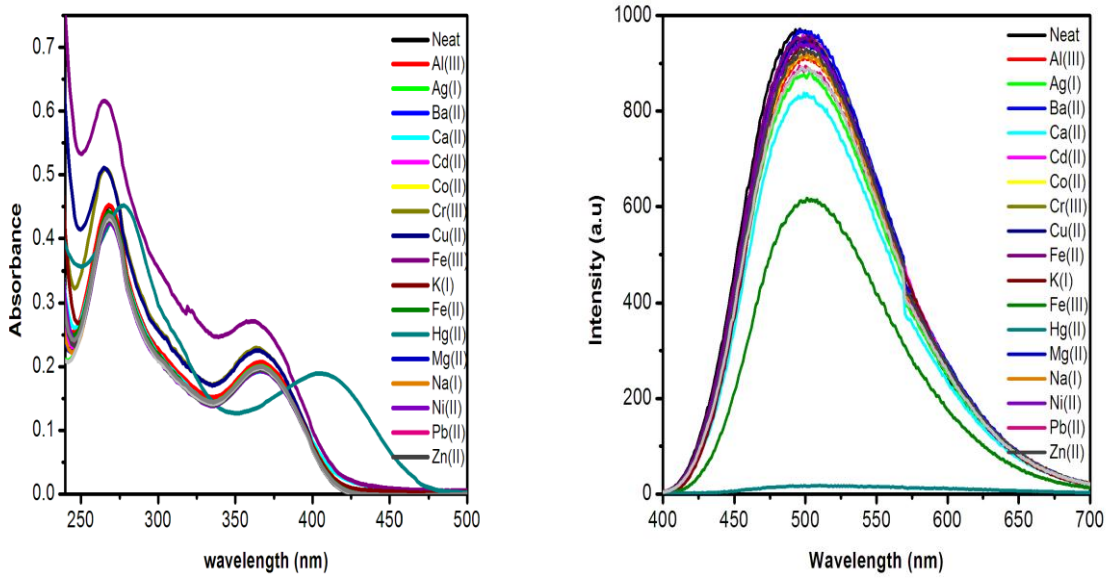

Figure S13.(i) Absorption spectra (10 μM) and (ii) fluorescence spectra (50 μM) of **PP4** in CH_3CN-H_2O (9:1, v/v) on addition of 10eq. of various metal cations (metal nitrates were studied).

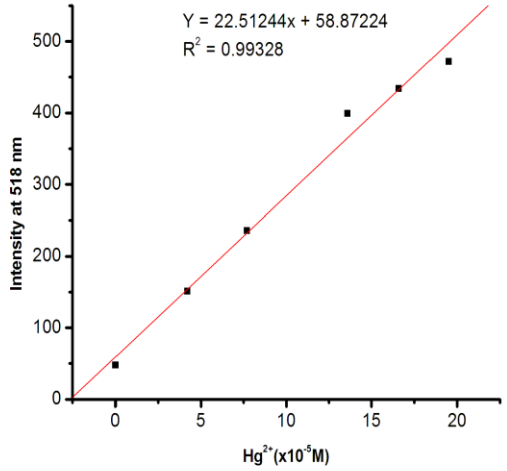

Figure S14. Determination of detection limit based on fluorescence intensity at 518 nm of **PP1**with Hg^{2+} (λ_{ex} = 356 nm). Linear equation = 22.51244x + 58.87224, R^2 = 0.99328, (S = 0.08560)

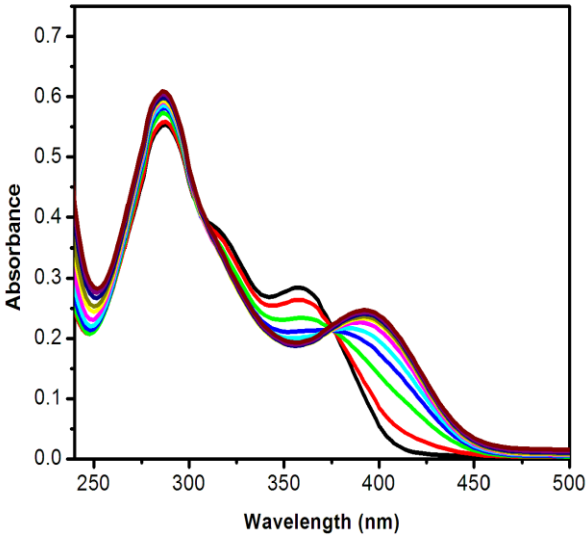

Figure S15. Absorptionspectraof probe **PP2** (10 μM) upon addition of increasing concentration (0-10 eq.) of Hg^{2+} in CH_3CN-H_2O (8:2, v/v).

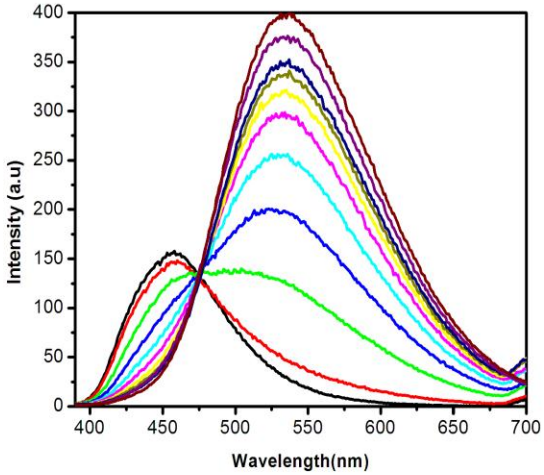

Figure S16. Fluorescence spectra of probe **PP2** (50 μM) upon addition of increasing concentration (0-4eq.) of Hg^{2+} in CH_3CN-H_2O (8:2, v/v).

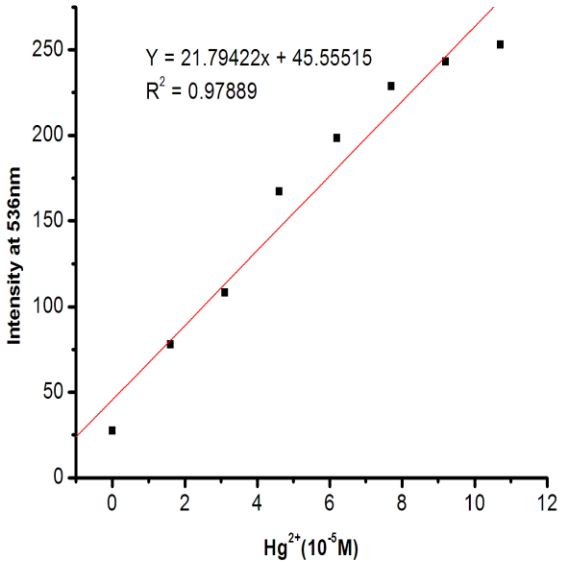

Figure S17. Determination of detection limit based on fluorescence intensity at 536 nm of **PP2** with Hg^{2+} (λ_{ex} = 358 nm). Linear equation = 21.79422x + 45.55515, R^2 = 0.97889, (S = 0.06937)

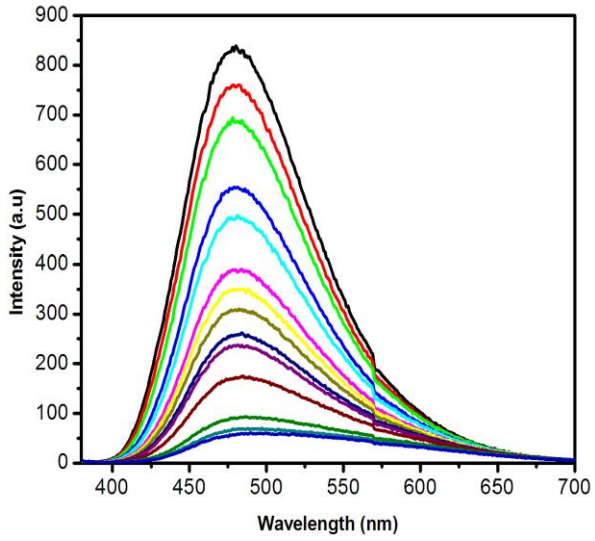

Figure S18. Fluorescence spectra of probe **PP3** (50 μM) upon addition of increasing concentration (0-4eq.) of Hg^{2+} in CH_3CN-H_2O (7:3, v/v).

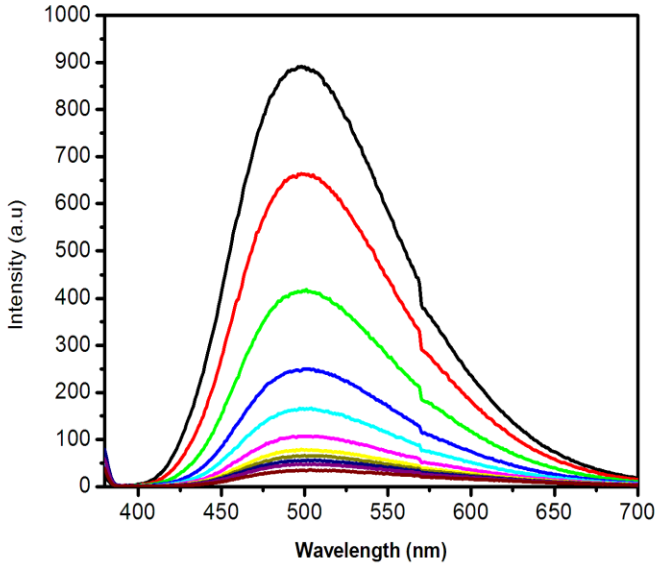

Figure S19. Fluorescence spectra of probe **PP4** (5 μM) upon addition of increasing concentration (0-2eq.) of Hg^{2+} in CH_3CN-H_2O (9:1, v/v).

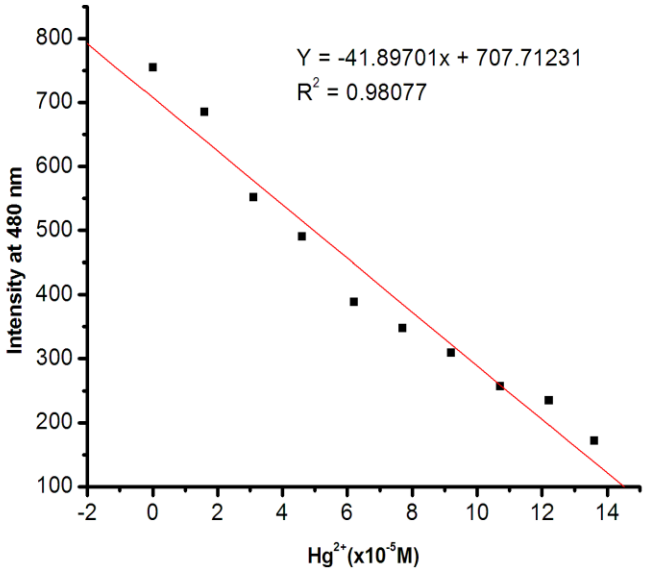

Figure S20. Determination of detection limit based on fluorescence intensity at 480 nm of **PP3** with Hg^{2+} (λ_{ex} = 364 nm). Linear equation = -41.89701x + 707.71231, R^2 = 0.98077, (S = 0.46900)

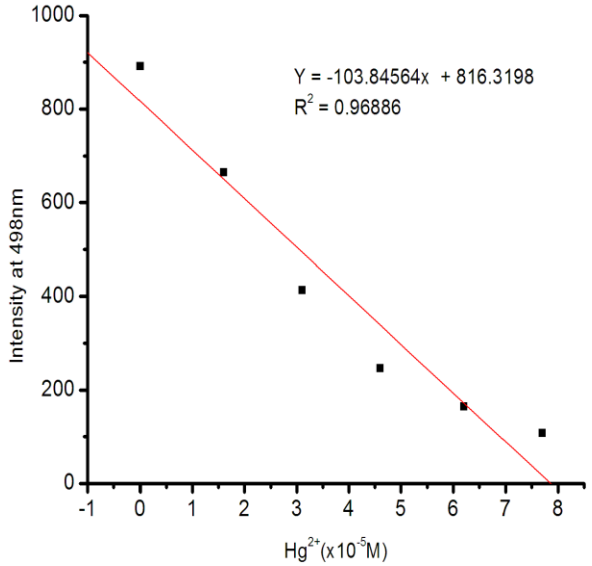

Figure S21. Determination of detection limit based on fluorescence intensity at 498 nm of **PP4** with Hg^{2+} (λ_{ex} = 368 nm). Linear equation = -103.84564x + 816.3198, R^2 = 0.96886, (S = 0.28300)

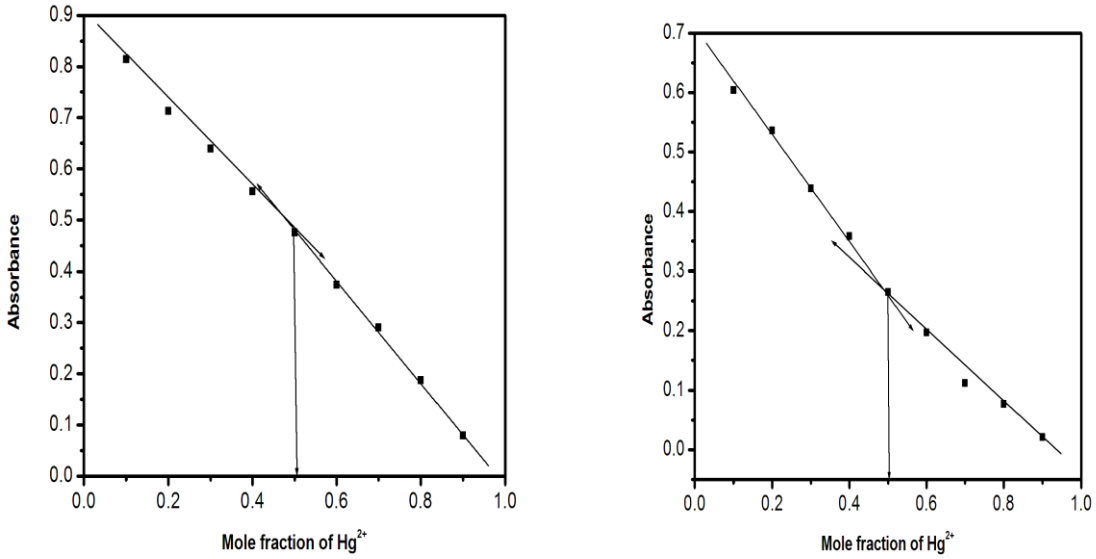

Figure S22. Job's plot for stoichiometric determination of probe (i) **PP3** and (ii) **PP4** Hg^{2+} ions.

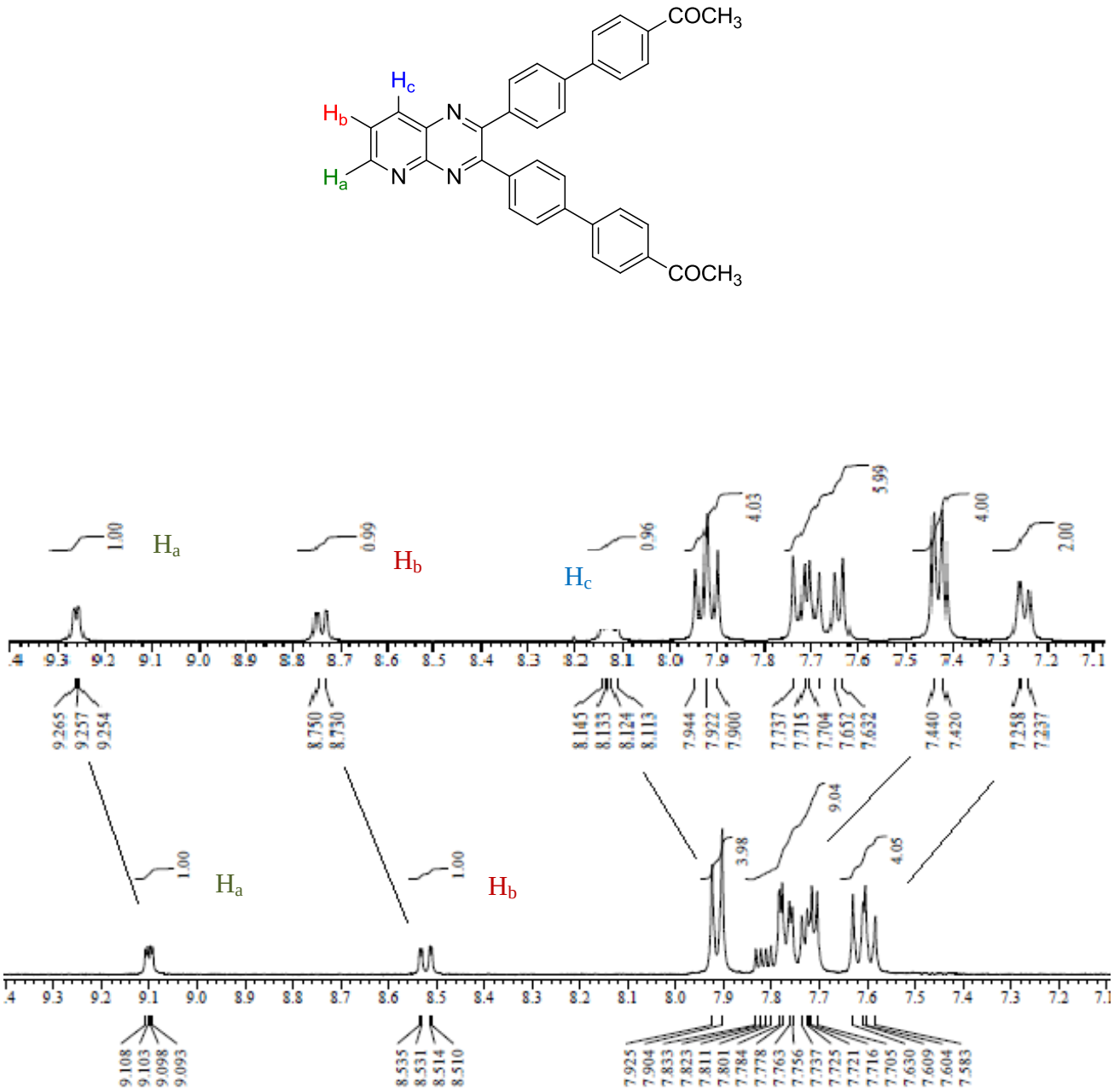

Figure S23. Partial ^{1}H NMR spectra of probe **PP2** in DMSO-d_6 (i) before and (ii) after addition of Hg^{2+} (1eq.).

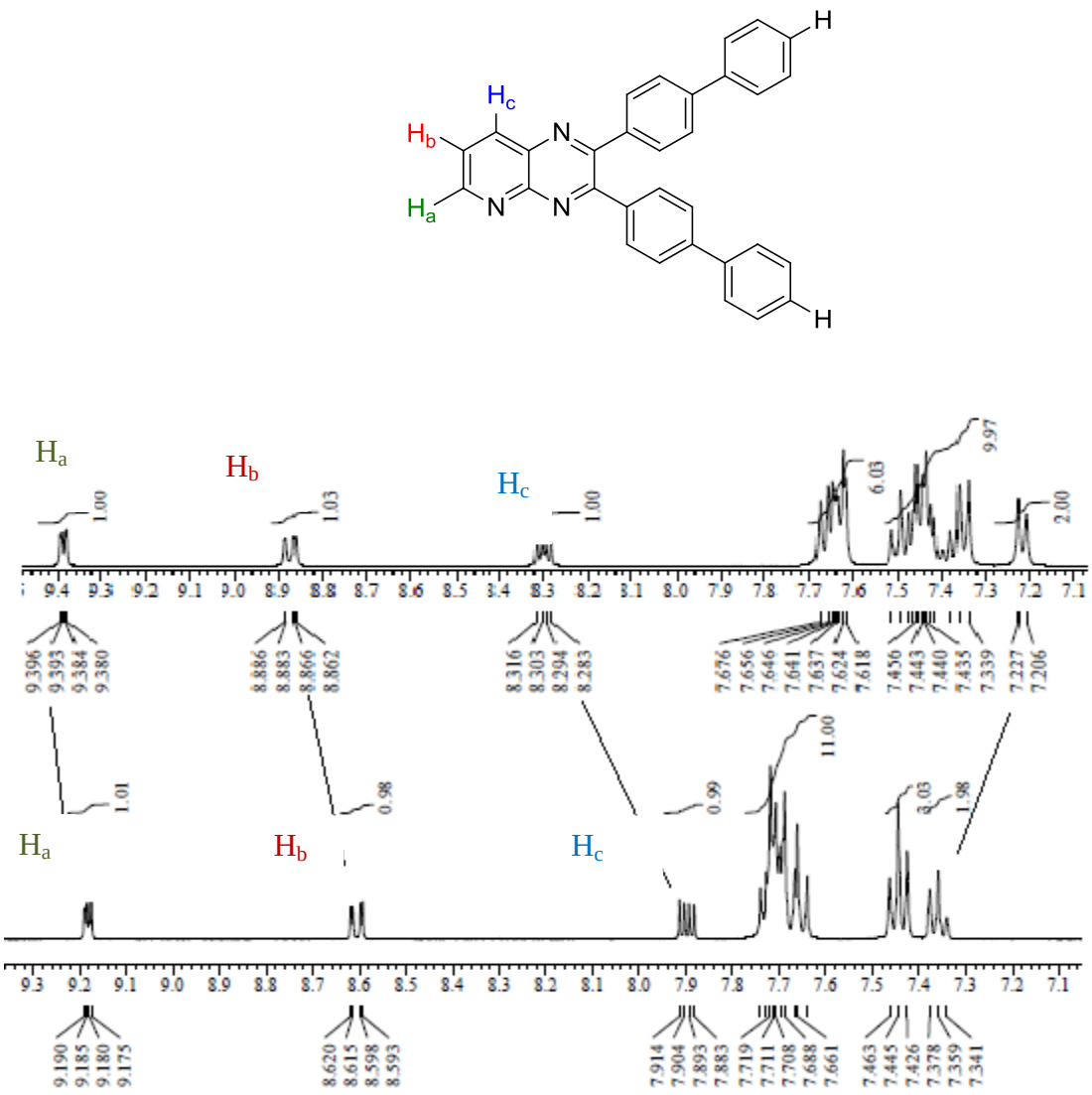

Figure S24. Partial ^{1}H NMR spectra of probe **PP3** in DMSO-d_6 (i) before and (ii) after addition of Hg^{2+} (1eq.).

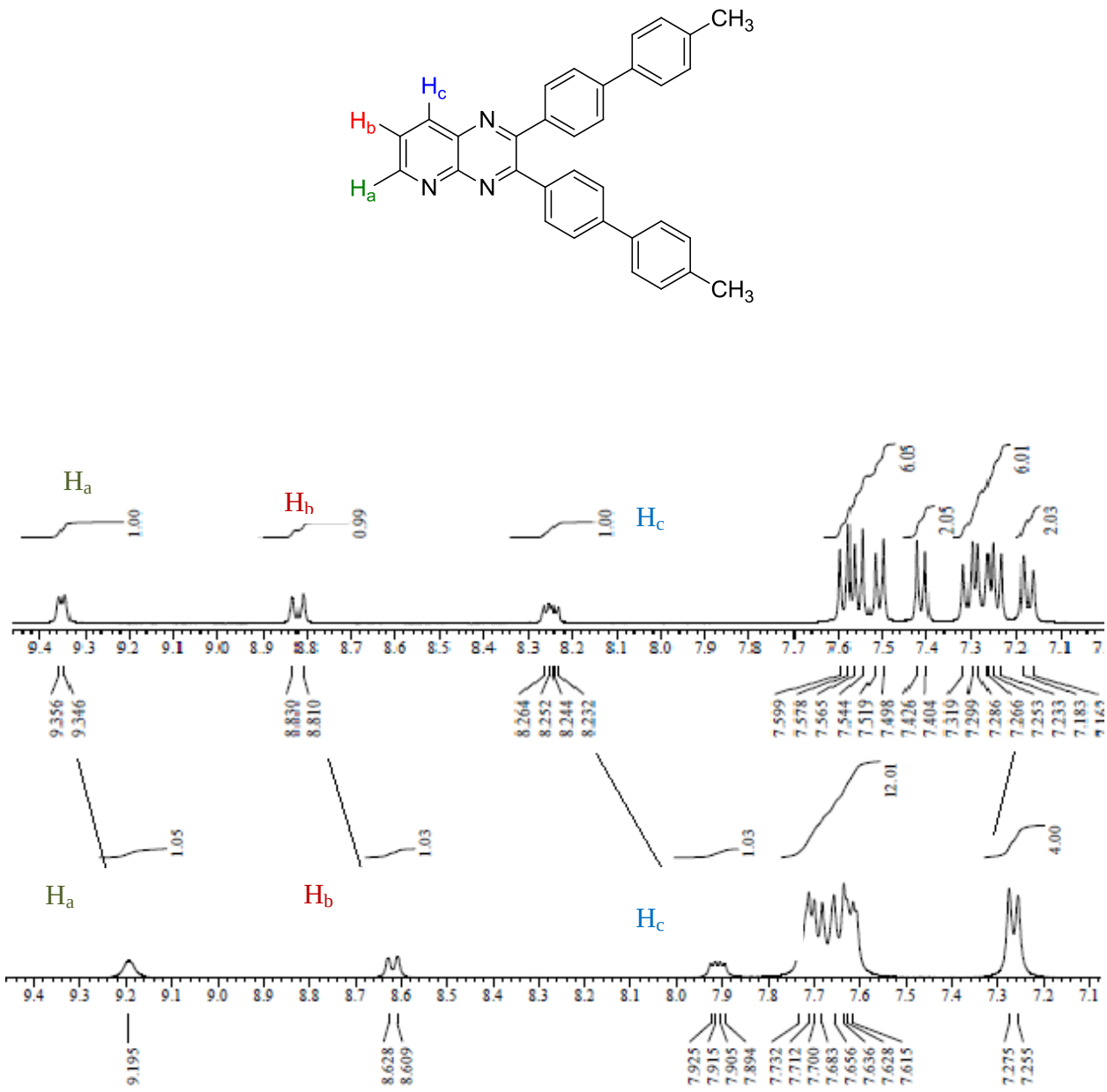

Figure S25. Partial ^{1}H NMR spectra of probe **PP4** in DMSO-d_6 (i) before and (ii) after addition of Hg^{2+} (1eq.).

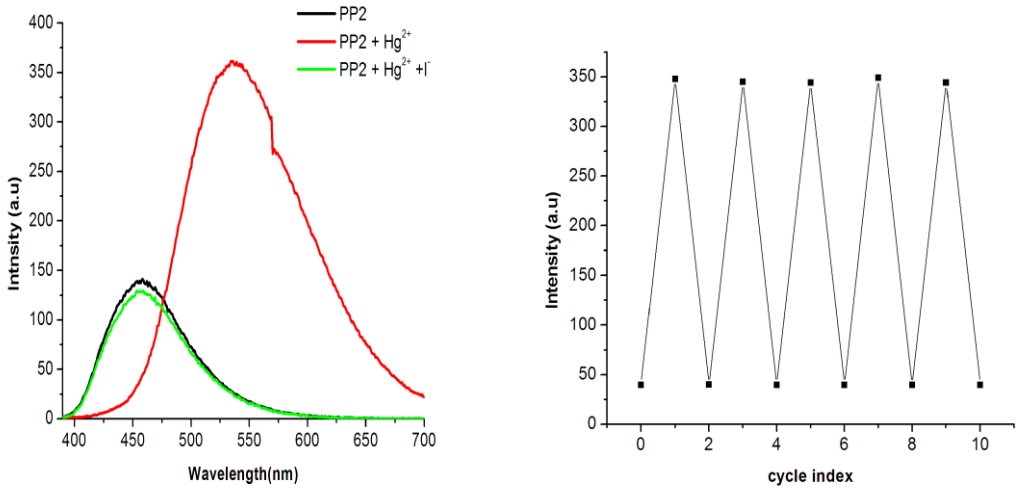

Figure S26. (i) Flourescence spectra of **PP2** in CH_3CN-H_2O (8:2, v/v) **PP2** + Hg^{2+}, **PP2** + Hg^{2+}+ I^- ii) Reversibility cycle of **PP2** (measured at λ_{emm} 536nm) after simultaneous addition of Hg^{2+} and I^-.

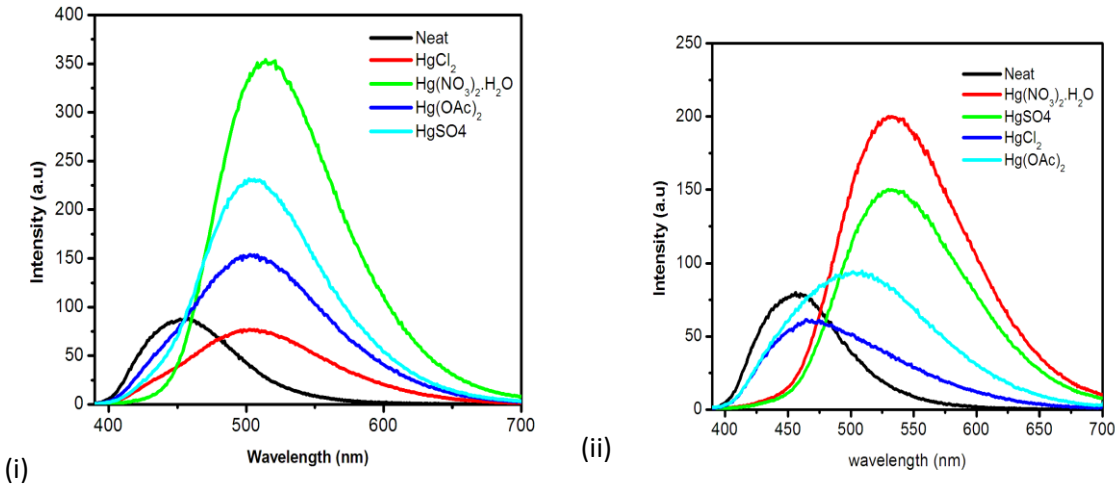

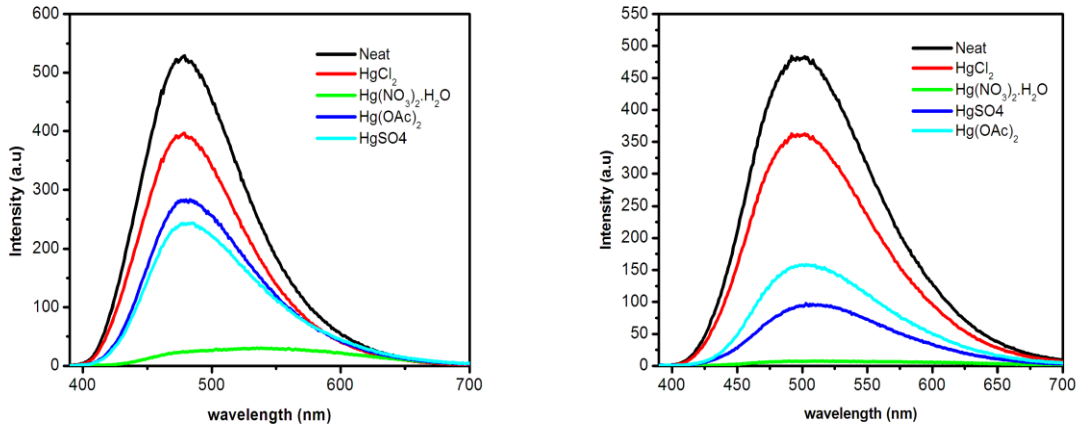

Figure S27. Fluorescence spectra of (i) **PP1** (ii) **PP2** (iii) **PP3** and (iv) **PP4** (50 μM) in the presence of Hg^{2+} with different counterions.

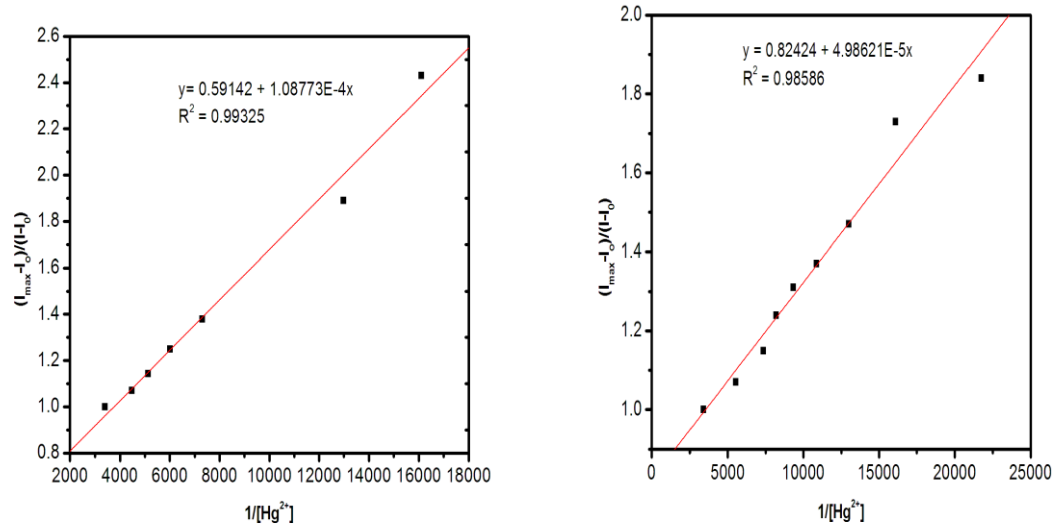

Figure S28. Benesi-Hildebrand plot for calculation of binding constant for complex formation between (i) **PP1** and Hg^{2+} (ii) **PP2** and Hg^{2+}.

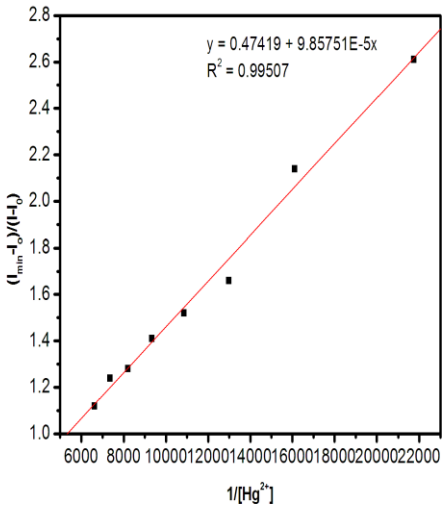

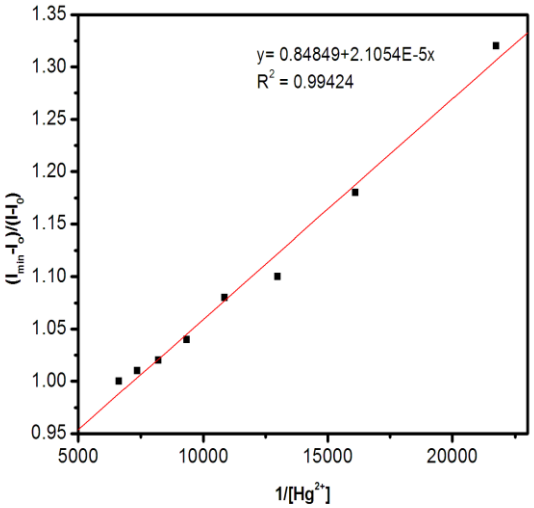

(i) **(ii)**

Figure S29. Benesi-Hildebrand plot for calculation of binding constant for complex formation between (i) **PP3** and Hg^{2+} (ii) **PP4** and Hg^{2+}.

Table S2. Comparison of proposed probes with previously reported chemosensors

Previous Literature	Solvent	Limit of detection
1. Applied Materials & Interfaces, 2010, 2, 1066[3]	THF	5×10^{-7} M
2. Spectrochimica Acta Part A, 2012, 93, 245[4]	DMSO	0.1 μM
3. Tetrahedron, 2013, 69, 1965[5]	CH_3CN/H_2O (4:1; V/V)	1.74 μM
4. Sensors and Actuators B, 2014, 196, 388[6]	Acetonitrile:Water 7:3	4.60 μM
5. Dyes and Pigments, 2015, 113, 763[7]	DMF/Water 1:1	2.20×10^{-6} M
6. Journal of Luminscence, 2016, 175, 182[8]	THF/H_2O (7/3; V/V)	3.952×10^{-7} M
7. Tetrahedron, 2017, 73, 2824[9]	THF/H_2O (99:1; V/V)	0.36 μM
8. Journal of Photochemistry and Photobiology A: Chemistry 2017, 332, 293[10]	THF/H_2O (99:1; V/V)	0.089 μM
9. This Work	Acetonitrile/water	
	PP1 (5:5; V/V)	1.14×10^{-7} M
	PP2 (8:2; V/V)	9.55×10^{-8} M
	PP3 (7:3; V/V)	3.37×10^{-7} M
	PP4 (9:1; V/V)	8.17×10^{-8} M

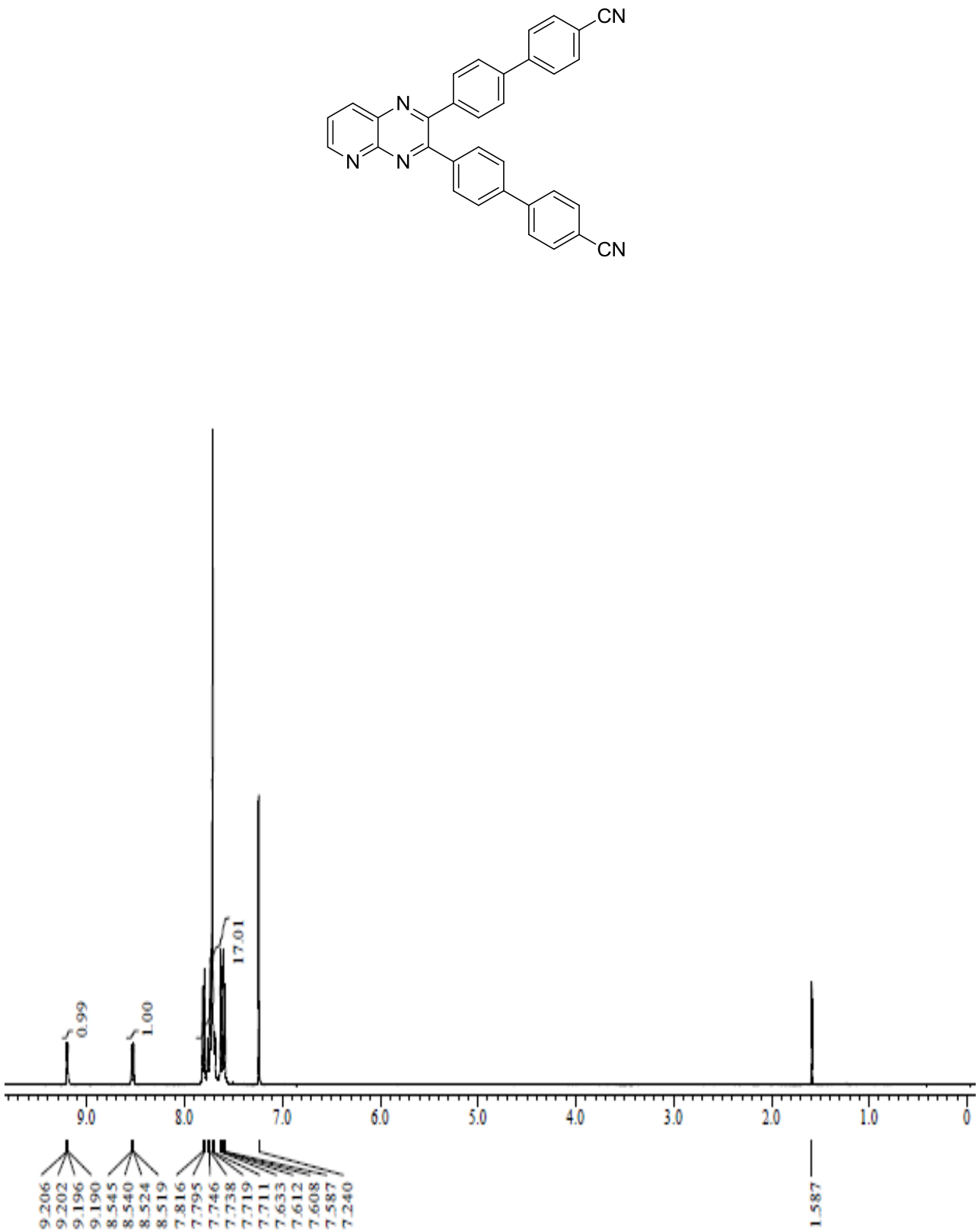

Figure S30. ^{1}H NMR (400 MHz, $CDCl_3$) spectrum of **PP1.**

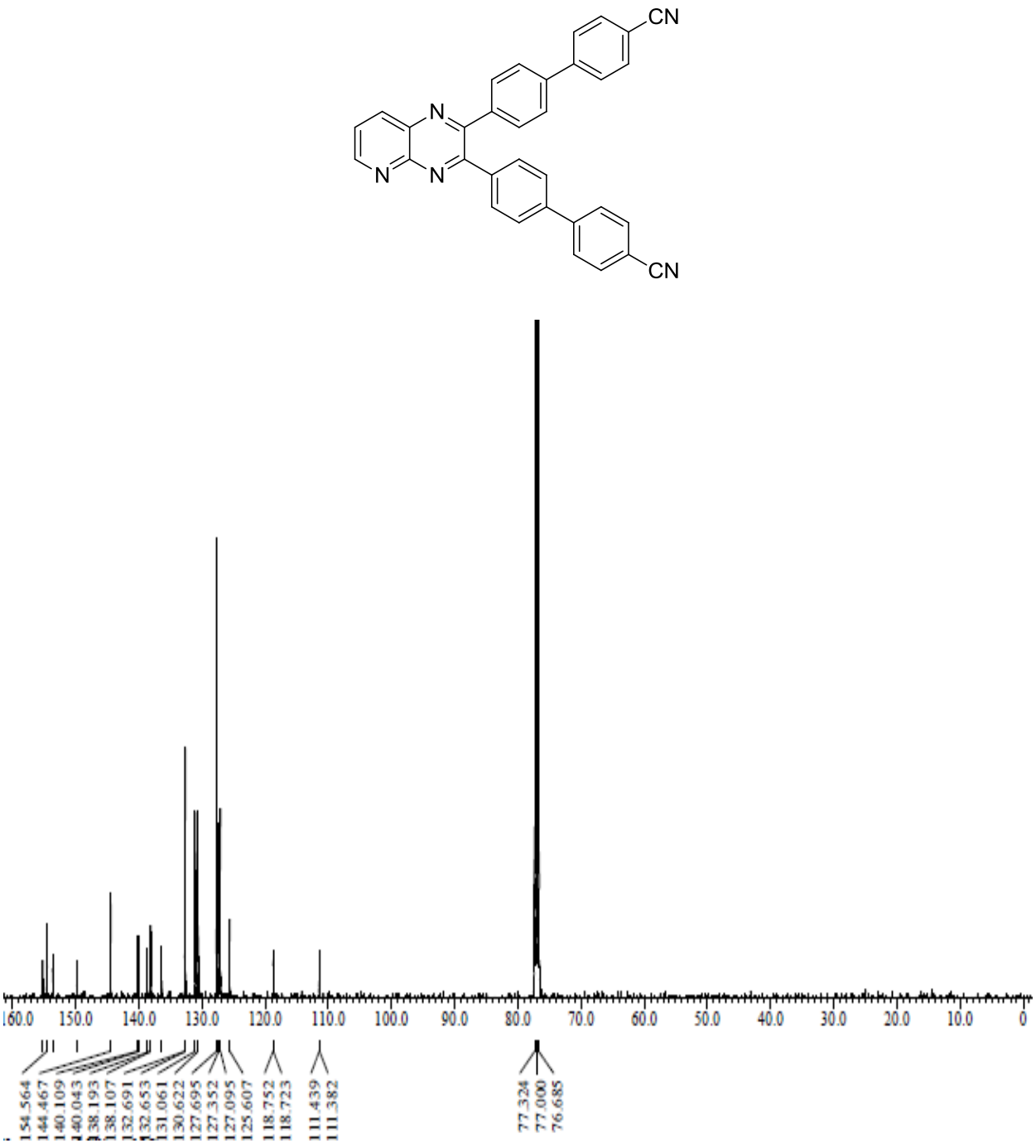

Figure S31. ^{13}C NMR (100 MHz, $CDCl_3$) spectrum of **PP1**.

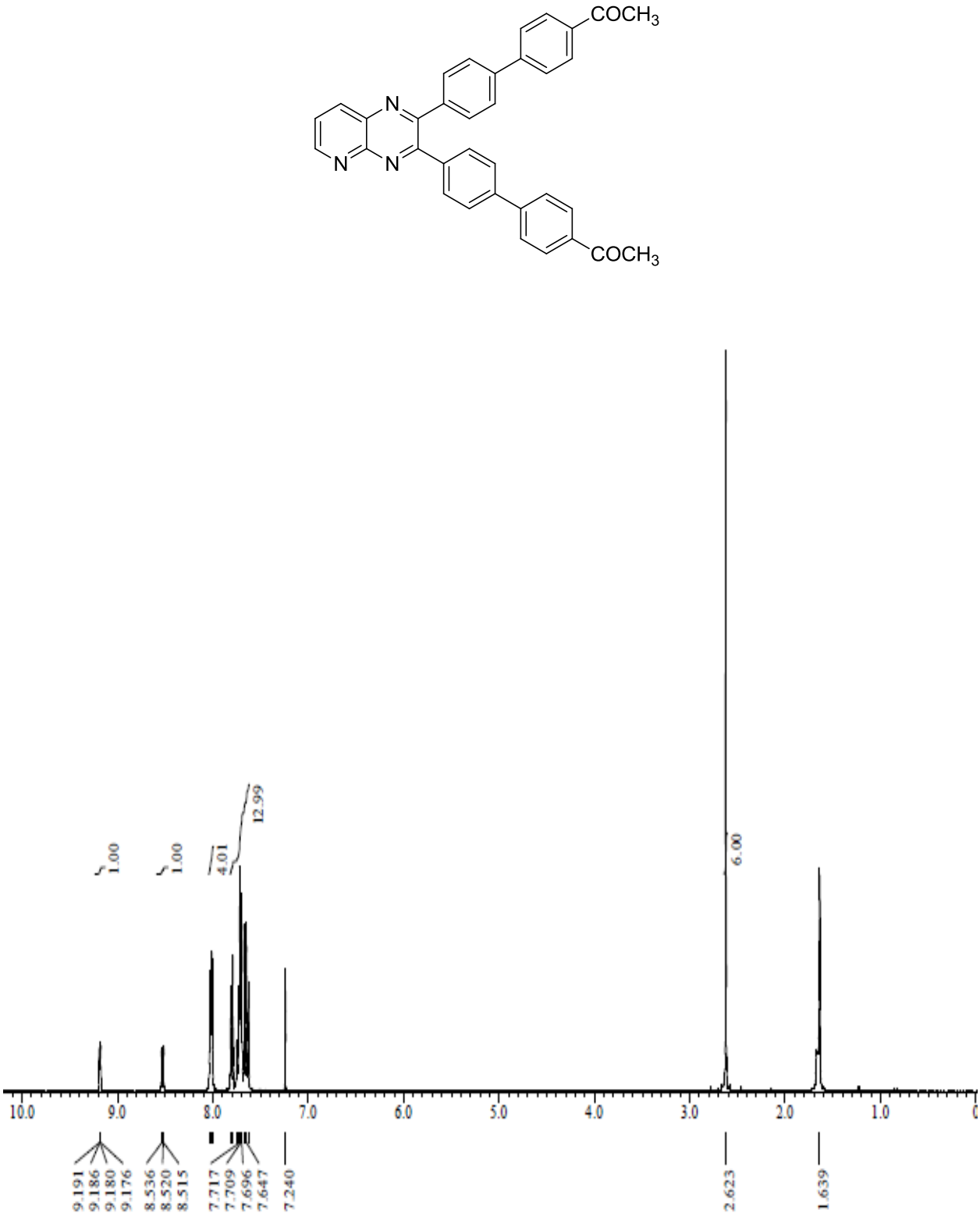

Figure S32. ^{1}H NMR (400 MHz, $CDCl_3$) spectrum of **PP2.**

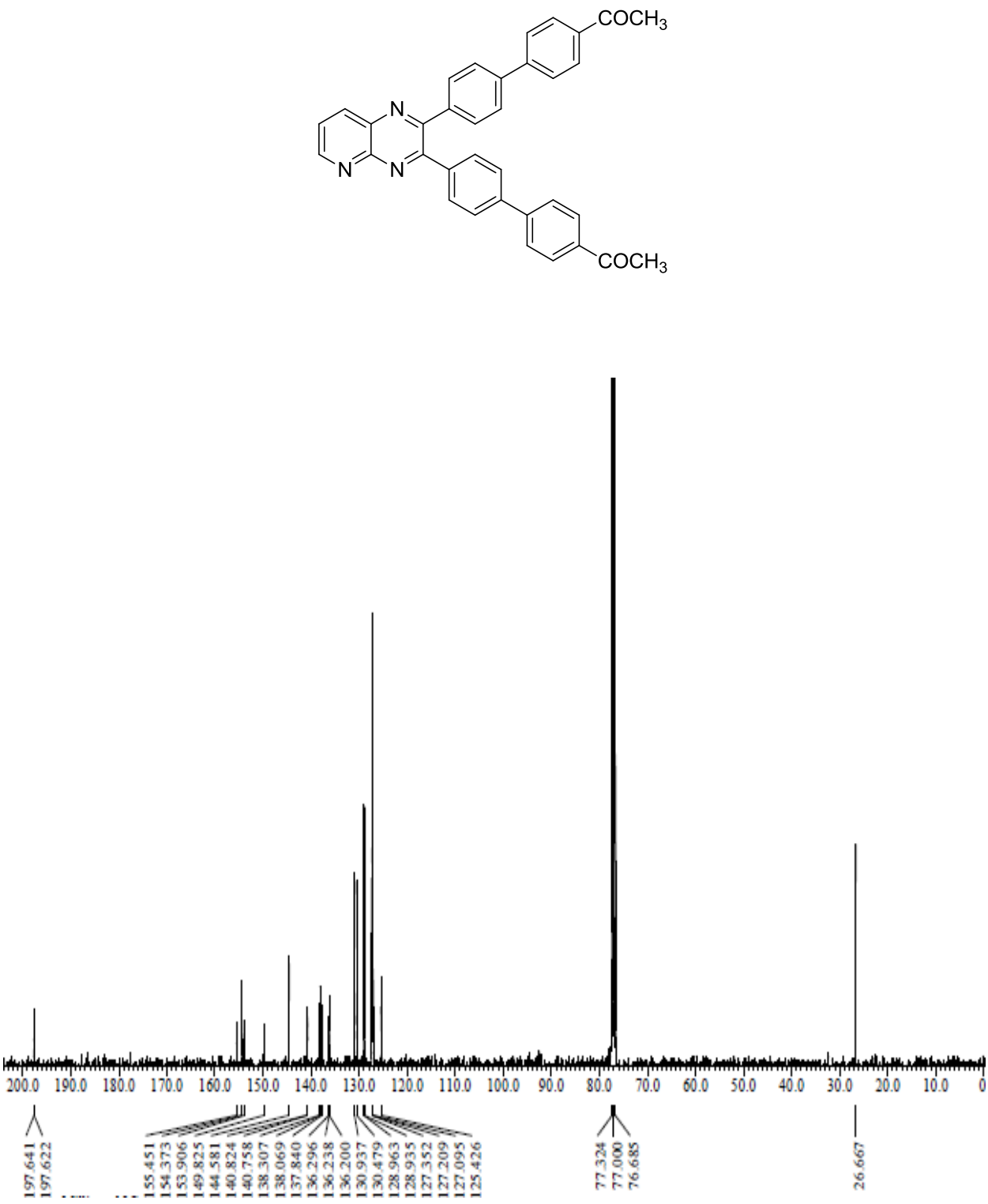

Figure S33. ^{13}C NMR (100 MHz, $CDCl_3$) spectrum of **PP2.**

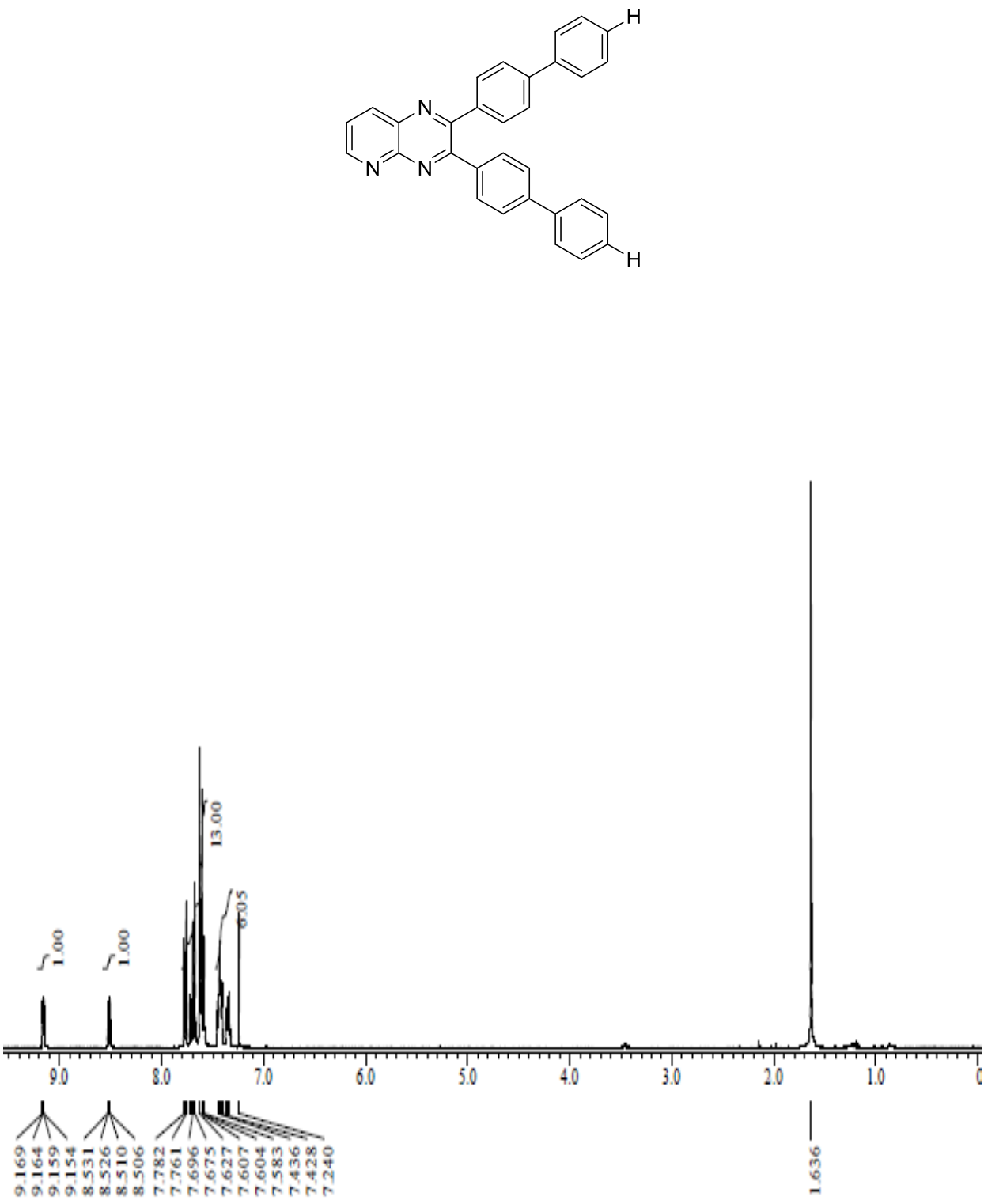

Figure S34. ^{1}H NMR (400 MHz, $CDCl_3$) spectrum of **PP3.**

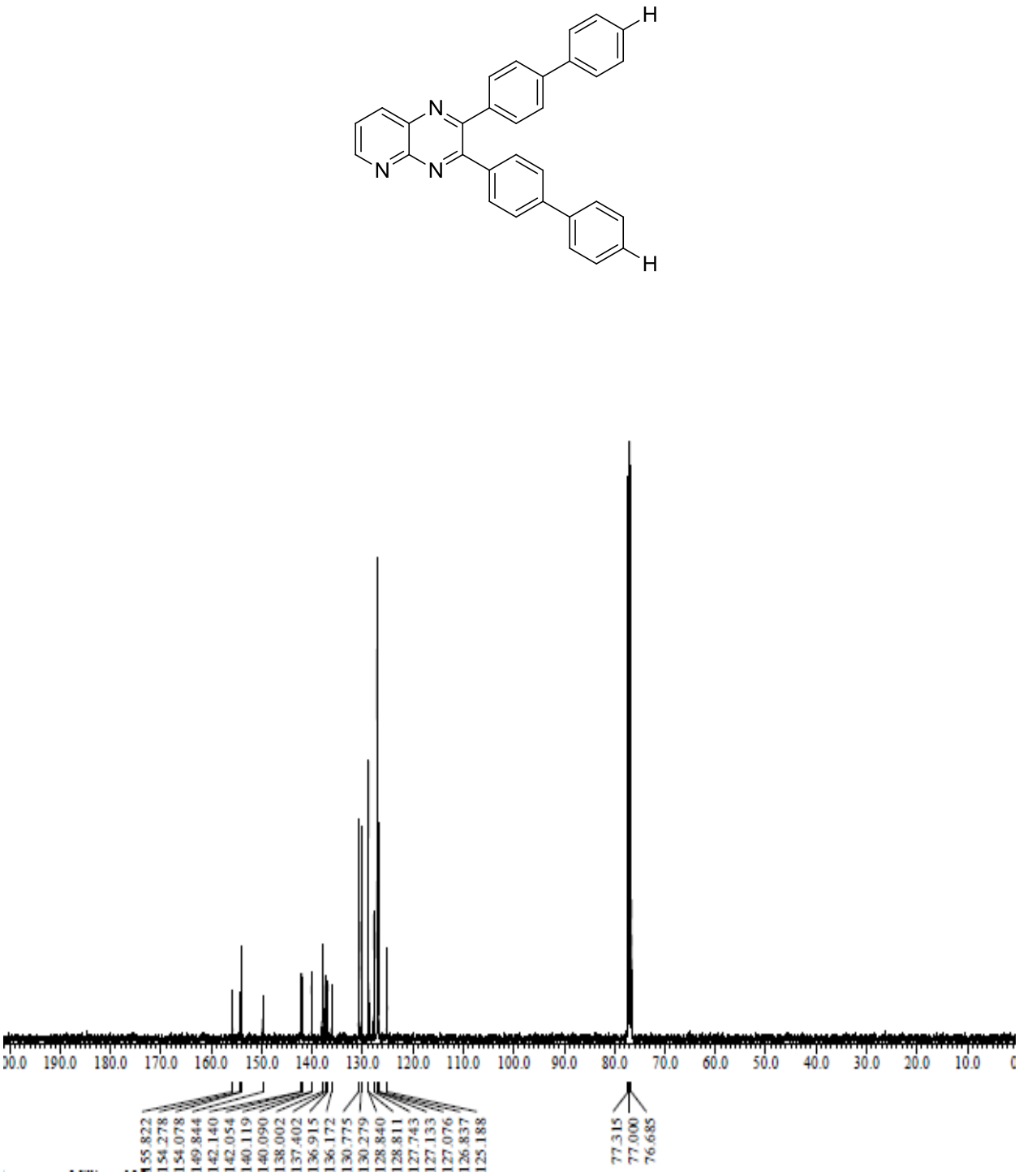

Figure S35. ^{13}C NMR (100 MHz, $CDCl_3$) spectrum of **PP3.**

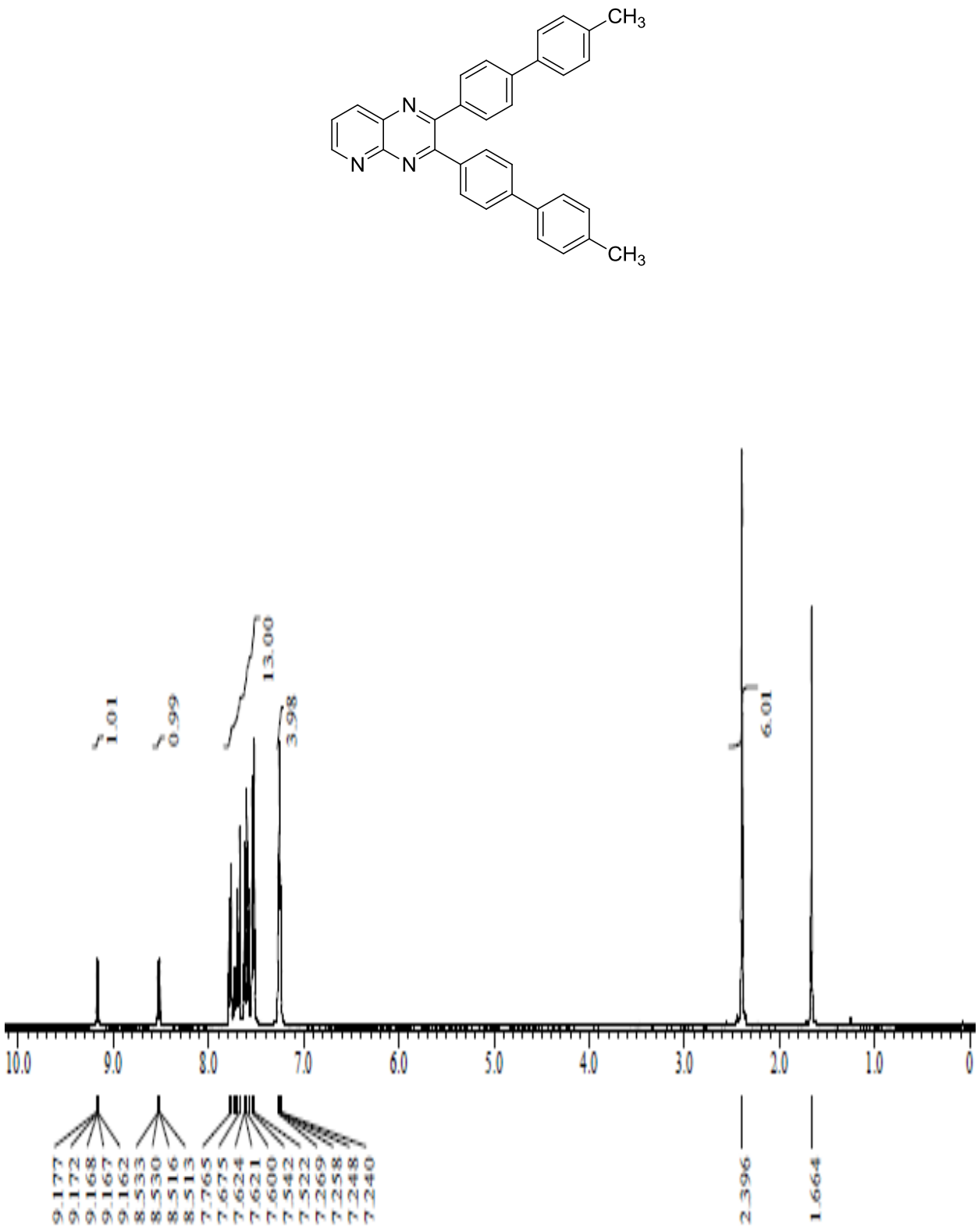

Figure S36. ^{1}H NMR (400 MHz, $CDCl_3$) spectrum of **PP4.**

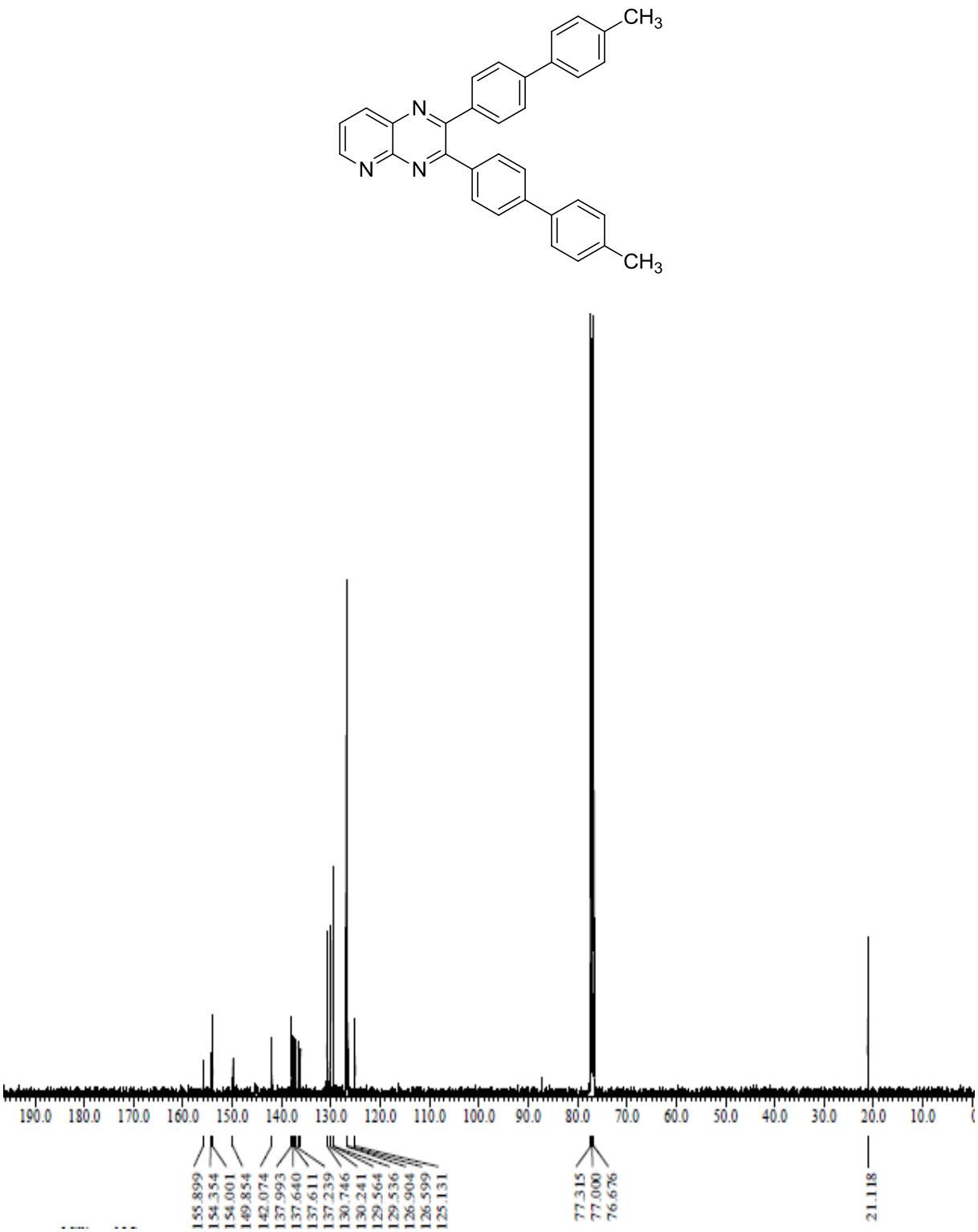

Figure S37. ^{13}C NMR (100 MHz, $CDCl_3$) spectrum of **PP4.**

Data File	GS-68P.d	**Sample Name**	GS-68P
Sample Type	Sample	**Position**	P1-E7
Instrument Name	Instrument 1	**User Name**	
Acq Method	29.10.2014.m	**Acquired Time**	06-09-2016 12:58:02
IRM Calibration Status	Success	**DA Method**	Default.m
Comment			

Sample Group **Info.**
Acquisition SW Version 6200 series TOF/6500 series Q-TOF B.05.01 (B5125)

Compound Table

Compound Label	RT	Mass	Formula	MFG Formula	MFG Diff (ppm)	DB Formula
Cpd 9: C33 H19 N5	11	485.1639	C33 H19 N5	C33 H19 N5	0.38	C33 H19 N5

Compound Label	*m/z*	RT	Algorithm	Mass
Cpd 9: C33 H19 N5	486.1711	11	Find by Molecular Feature	485.1639

MFE MS Spectrum

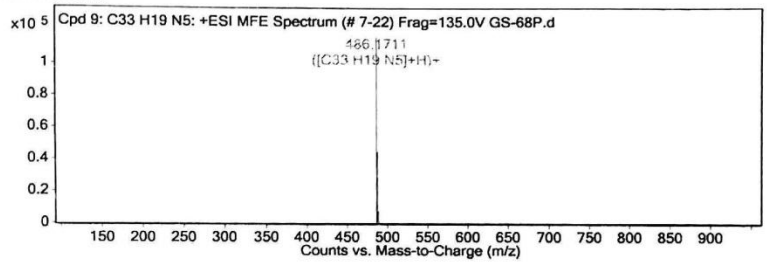

MFE MS Zoomed Spectrum

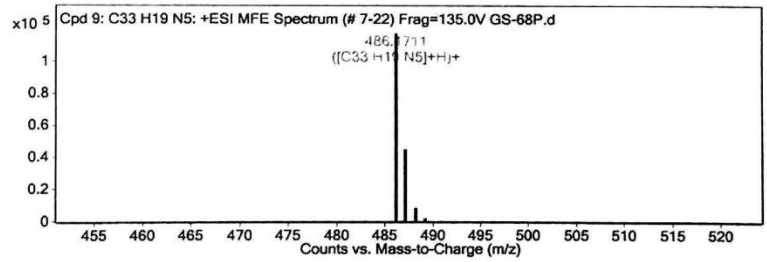

MS Spectrum Peak List

m/z	z	Abund	Formula	Ion
486.1711	1	117433.75	C33 H19 N5	(M+H)+
487.1742	1	44651.36	C33 H19 N5	(M+H)+
488.1772	1	8005.28	C33 H19 N5	(M+H)+
489.1827	1	1089.34	C33 H19 N5	(M+H)+

--- End Of Report ---

Figure S38. HRMS data of **PP1.**

Data File	GS-125P.d	**Sample Name**	GS-125P
Sample Type	Sample	**Position**	P1-C2
Instrument Name	Instrument 1	**User Name**	
Acq Method	29.10.2014.m	**Acquired Time**	24-05-2017 13:43:57
IRM Calibration Status	[redacted]	**DA Method**	Default.m
Comment			

Sample Group **Info.**

Acquisition SW Version	6200 series TOF/6500 series Q-TOF B.05.01 (B5125)

Compound Table

Compound Label	RT	Mass	Formula	MFG Formula	MFG Diff (ppm)	DB Formula
Cpd 10: C35 H25 N3 O2	11	519.1956	C35 H25 N3 O2	C35 H25 N3 O2	-1.83	C35 H25 N3 O2

Compound Label	*m/z*	RT	Algorithm	Mass
Cpd 10: C35 H25 N3 O2	520.2037	11	Find by Molecular Feature	519.1956

MFE MS Spectrum

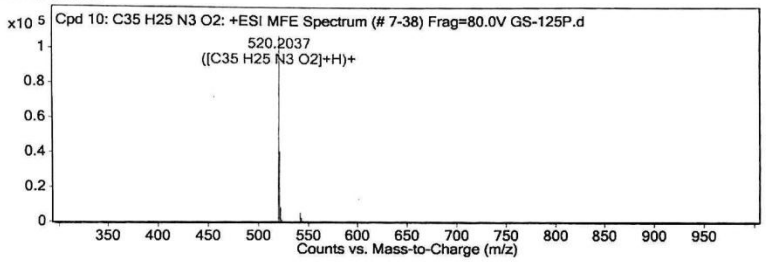

MFE MS Zoomed Spectrum

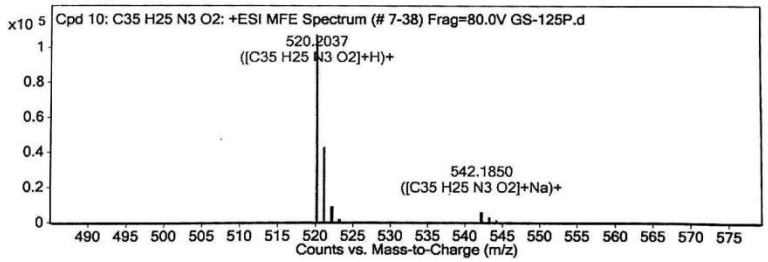

MS Spectrum Peak List

m/z	z	Abund	Formula	Ion
520.2037	1	107599.23	C35 H25 N3 O2	(M+H)+
521.2068	1	40720.06	C35 H25 N3 O2	(M+H)+
522.2107	1	8536.36	C35 H25 N3 O2	(M+H)+
523.2155	1	1276.29	C35 H25 N3 O2	(M+H)+
524.2289	1	119.44	C35 H25 N3 O2	(M+H)+
542.185	1	5215.81	C35 H25 N3 O2	(M+Na)+
543.1876	1	1978.92	C35 H25 N3 O2	(M+Na)+
544.1908	1	494.43	C35 H25 N3 O2	(M+Na)+

--- End Of Report ---

Figure S39. HRMS data of **PP2.**

Qualitative Compound Report

Data File	GS-138.d	**Sample Name**	GS-138
Sample Type	Sample	**Position**	P1-A6
Instrument Name	Instrument 1	**User Name**	
Acq Method	29.10.2014.m	**Acquired Time**	25-09-2017 14:50:47
IRM Calibration Status	Success	**DA Method**	Default.m
Comment			

Sample Group **Info.**
Acquisition SW Version 6200 series TOF/6500 series Q-TOF B.05.01 (B5125.1)

Compound Table

Compound Label	RT	Mass	Formula	MFG Formula	MFG Diff (ppm)	DB Formula
Cpd 10: C31 H21 N3	7	435.1732	C31 H21 N3	C31 H21 N3	0.86	C31 H21 N3

Compound Label	*m/z*	RT	Algorithm	Mass
Cpd 10: C31 H21 N3	436.1805	7	Find by Molecular Feature	435.1732

MFE MS Spectrum

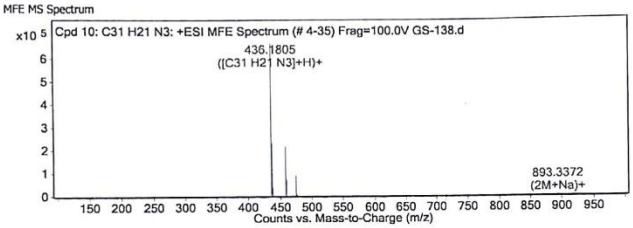

MFE MS Zoomed Spectrum

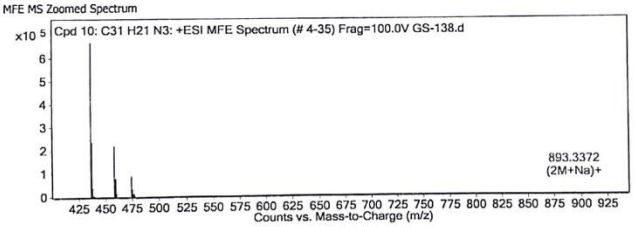

MS Spectrum Peak List

m/z	z	Abund	Formula	Ion
436.1805	1	668102.94	C31 H21 N3	(M+H)+
437.1835	1	232725.29	C31 H21 N3	(M+H)+
438.187	1	38773.45	C31 H21 N3	(M+H)+
439.1905	1	4924.56	C31 H21 N3	(M+H)+
458.1621	1	218552.67	C31 H21 N3	(M+Na)+
459.1652	1	73853.01	C31 H21 N3	(M+Na)+
460.1672	1	12583.37	C31 H21 N3	(M+Na)+
474.1358	1	87992.23	C31 H21 N3	(M+K)+
475.1394	1	29047.98	C31 H21 N3	(M+K)+
476.1378	1	11271.06	C31 H21 N3	(M+K)+

--- End Of Report ---

Agilent Technologies Page 1 of 1 Printed at: 14:54 on:25-09-2017

Figure S40. HRMS data of **PP3.**

Qualitative Compound Report

Data File	GS-120P.d	**Sample Name**	GS-120P
Sample Type	Sample	**Position**	P1-D2
Instrument Name	Instrument 1	**User Name**	
Acq Method	29.10.2014.m	**Acquired Time**	21-04-2017 14:02:47
IRM Calibration Status	Success	**DA Method**	Default.m
Comment			

Sample Group **Info.**
Acquisition SW Version 6200 series TOF/6500 series Q-TOF B.05.01 (B5125)

Compound Table

Compound Label	RT	Mass	Formula	MFG Formula	MFG Diff (ppm)	DB Formula
Cpd 10: C33 H25 N3	10	463.2051	C33 H25 N3	C33 H25 N3	-0.6	C33 H25 N3

Compound Label	*m/z*	RT	Algorithm	Mass
Cpd 10: C33 H25 N3	464.2124	10	Find by Molecular Feature	463.2051

MFE MS Spectrum

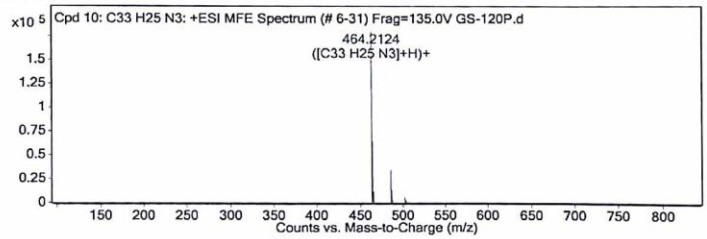

MFE MS Zoomed Spectrum

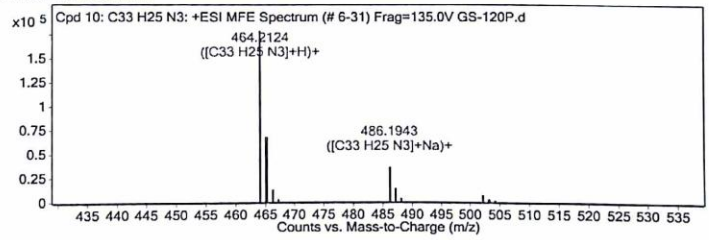

MS Spectrum Peak List

m/z	z	Abund	Formula	Ion
464.2124	1	179318.75	C33 H25 N3	(M+H)+
465.2155	1	64742.68	C33 H25 N3	(M+H)+
466.2183	1	11788.65	C33 H25 N3	(M+H)+
467.2237	1	1728.36	C33 H25 N3	(M+H)+
486.1943	1	34243.7	C33 H25 N3	(M+Na)+
487.1969	1	13316.4	C33 H25 N3	(M+Na)+
488.2015	1	2441.08	C33 H25 N3	(M+Na)+
502.167	1	5859.67	C33 H25 N3	(M+K)+
503.1703	1	2342.77	C33 H25 N3	(M+K)+
504.1704	1	886.26	C33 H25 N3	(M+K)+

--- End Of Report ---

Figure S41. HRMS data of **PP4.**

1. S. Madhu, D. K. Sharma, S. K. Basu, S. Jadhav, A. Chowdhury and M. Ravikanth, *Inorg. Chem.*, 2013, **52**, 11136-11145.
2. Y. Fang, X. Li, J.-Y. Li, G.-Y. Wang, Y. Zhou, N.-Z. Xu, Y. Hu and C. Yao, *Sens. Actuators B Chem.*, 2018, **255**, 1182-1190.
3. X. Cheng, Q. Li, J. Qin and Z. Li, *ACS Appl. Mater. Interfaces*, 2010, **2**, 1066-1072.
4. J. Liu, M. Yu, X.-C. Wang and Z. Zhang, *Spectrochim. Acta. A. Mol. Biomol. Spectrosc.*, 2012, **93**, 245-249.
5. H.-F. Wang and S.-P. Wu, *Tetrahedron*, 2013, **69**, 1965-1969.
6. S. Lee, B. A. Rao and Y.-A. Son, *Sens. Actuators B Chem.*, 2014, **196**, 388-397.
7. S. Malkondu and S. Erdemir, *Dyes Pigments*, 2015, **113**, 763-769.
8. X. Wu, Q. Niu, T. Li, Y. Cui and S. Zhang, *J. Lumin.*, 2016, **175**, 182-186.
9. Q. Zhang, J. Zhang, H. Zuo, C. Wang and Y. Shen, *Tetrahedron*, 2017, **73**, 2824-2830.
10. 1Q. Zhang, Y. Li, H. Zuo, C. Wang and Y. Shen, *J. Photochem. Photobiol. Chem.*, 2017, **332**, 293-298.